

Breakdown Formation in a Transient Hollow Cathode Discharge—A Statistical Study

P. Choi, H. Chuaqui, M. Favre, and V. Colas

Abstract—Discharge formation at low pressure is found to be greatly influenced in the presence of a suitable hollow cathode region. The formation of a moving virtual anode which extends the anode potential to within the hollow cathode region is thought to be responsible for the enhanced ionization growth which subsequently leads to gas breakdown. In this paper, the spatial evolution of the local potential in the discharge region of a pulsed hollow cathode discharge has been measured in a range of pressures with two different cathode apertures. An extensive data set has been collected and analyzed using a statistical technique. From the characteristic of the statistical distribution of the data, unique features associated with the role of hollow cathode at the different stages of discharge formation have been identified. It was found that the influence of the hollow cathode region is strongest in the start of ionization growth and in the final change over to high current breakdown.

I. INTRODUCTION

BREAKDOWN formation at low pressure, when collisional processes are not effective, relies on a number of secondary processes. This is particularly important at high reduced electric field, E/N , conditions where secondary ionization processes take place primarily on the electrodes. When an aperture is introduced into the cathode, a hollow cathode region (HCR) is created behind the main discharge region (A-K gap). In the presence of a suitable HCR, the ionization growth in the main discharge region is found to be significantly modified and much enhanced. Inside the HCR, the electric field is low and is defined by the penetration of the field from the A-K gap, through the small aperture in the cathode. The lower E/N condition creates a very different ionization condition to that in the A-K gap. The geometry of the hollow cathode concentrates the electrons produced inside the HCR as they are continuously extracted, by the intrinsic electric field configuration, through the cathode aperture into the main discharge volume. Simulation has shown that the enhanced electron injection rate leads to the formation of a plasma region in the A-K gap, first near to the anode and then extending to the cathode, creating effectively a moving virtual anode,

which brings the applied voltage close to the cathode and enhances the leakage field within the HCR [1]. The existence of this virtual anode was measured experimentally [2]. The electron extraction into the A-K gap leaves behind in the HCR a region rich in ions. Part of the ions created in the A-K gap will also return through the aperture into the HCR after gaining energy from the applied field. This produces a region of enhanced positive space charge and subsequently the creation of a highly localized region of highly ionized plasma, at a location behind the cathode aperture, from which a large electron beam is extracted into the A-K gap. This effect is observed in simulation [3] and in experiment [4], [5]. The injection of a high current density electron beam leads to the formation of a highly conducting channel and thus breakdown. Devices like the pseudospark and the back-lit thyratron all exhibit these unique properties of the transient hollow cathode discharge (THCD) leading to the rapid breakdown in switching applications and in sources of high intensity, high brightness electron beams [6], [7].

The presence of an effective hollow cathode region thus modifies significantly the randomness in the breakdown statistics in low pressure discharges. This was investigated in a previous study which identifies the effectiveness of the hollow cathode in terms of the overall behavior of the breakdown statistics [8]. The qualitative picture introduced above on the breakdown formation process in the THCD, however, suggests that the causal relationship between the processes within the HCR, the formation of the virtual anode and the subsequent breakdown formation could be further clarified through their contribution and influences to the breakdown statistics.

In this paper, an extensive set of data has been collected to investigate the statistical distribution of the time of occurrence of different parts of the ionization growth and breakdown formation mechanisms in the THCD process. The statistics allow us to clarify some conditions which could be used to interpret the processes of breakdown formation and their time evolution, which are uniquely related to the role of the hollow cathode in discharge formation.

II. EXPERIMENTAL DETAILS

Discharge formation in nitrogen at 10 kV was studied with two different cathode apertures, 3 and 5 mm, with an aperture length of 6 mm. Anode-cathode separation was kept at 10 cm. The cathode electrode material was stainless steel. The pressure range covered spans from 60–400 mTorr. The discharge was operated at a repetition rate of 1 second to partially reduce the randomness in ionization growth, through the additional

Manuscript received August 15, 1994; revised March 19, 1995. The work was supported in part under a CEC SCIENCE contract No. SC1*CT910749 and CEC ISC contract No. C11*CT920053, and in part under FONDECYT No. 1930575.

P. Choi was with Blackett Laboratory, Imperial College of Science, Technology and Medicine, London SW7 2BZ, UK. He is now with LPMI, Ecole Polytechnique, Palaiseau 91128 CEDEX, France.

H. Chuaqui and M. Favre are with the Facultad de Física, Pontificia Universidad Católica de Chile, Casilla 306, Santiago 22, Chile.

V. Colas was with Ecole Supérieure des Procédés Electroniques et Optiques at the Université d'Orléans, 45067 Orleans, France.

IEEE Log Number 9412760.

effects of metastables [9]. The discharge apparatus uses a pulse charged plate capacitor to produce a high voltage step across the electrodes with a rise time of less than 50 ns, and a self-decay time constant of over 1 second. The voltage on the plate capacitor is transferred from a storage capacitor through a triggered spark gap and a light signal collected from the spark gap is used to mark the start of the voltage rise. Further details of the experimental apparatus can be found elsewhere [4], [10].

A capacitive probe array was developed to monitor the spatial evolution of electric potential and space charge in the ionizing medium [11]. Each probe in the array consists of a narrow conducting ring coaxial with the discharge tube. The rings couple capacitively to the inter electrode plasma. For the conditions in the present experiments the probe response is proportional to the time derivative of the product between the plasma potential and the coupling capacitance of the probe relative to the plasma. The probe array has been used successfully to identify the presence and movement of the virtual anode in a THCD. In this paper, six probes arranged as three pairs were used in the A-K gap, and two were placed inside the HCR. The probe signals were simultaneously recorded with a multichannel fast transient digitizer.

III. EXPERIMENTAL RESULTS

The total delay to breakdown from the application of the high voltage is divided nominally into a number of time intervals in connection with the capacitive probe array: 1) τ_A , the time interval between voltage rise and peak of signal from probe No. 1 (closest to the anode, at 24 mm from the anode face), 2) τ_B , the time interval between peak signals from probe No. 1 and probe No. 4 (at 57 mm from the anode face), 3) τ_C , the time interval between peak signals from probe No. 4 and probe No. 6 (closest to the cathode at 81 mm from the anode face) and, 4) τ_D , the time interval between peak of signal in probe No. 6 and electric breakdown (rise of the main discharge current). At each pressure and hollow cathode condition, a total of 128 sequential records were taken automatically by the data acquisition system under the control of a Personal Computer, at roughly 3 seconds interval per records. To visualize the data, the cumulative probability of these time intervals were plotted using the von Laue formalism [8], [12]. To establish that the 128 records would be sufficient to define the statistics, a number of 512 record samples were taken under different operating conditions for comparison. No significant deviation in the statistical behavior was found in the shorter records.

Fig. 1 shows typical data as recorded by the capacitive probes for 3 mm aperture at 150 mTorr pressure. Electric breakdown coincides with the first large negative excursion and subsequent oscillation seen in the probes corresponds to ringing in the discharge circuit. The rise and fall of the probe signals in the A-K gap is indicative of the establishment of a local potential in the vicinity of the probes. The presence of this potential is observed to occur later for the probe closer to the cathode. The unipolar nature of this signal shows the establishment of a spatial potential, which is interpreted as the virtual anode. [2]. The time evolution of the different probe

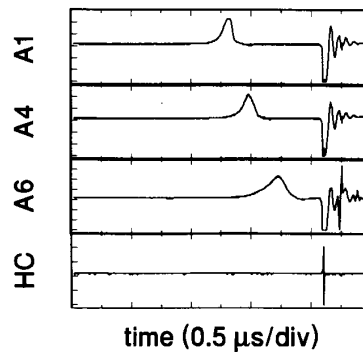


Fig. 1. Typical data recorded by the capacitive probe array for a 3 mm diameter aperture cathode at 150 mTorr operating pressure. The positions of the probes measured from the anode are: A1–24 mm, A4–57 mm and A6–81 mm. Probe HC is located inside the hollow cathode region close to the back of the cathode.

signals thus represents the movement of the virtual anode. The probe located inside the HCR shows a bipolar signal around the onset of full electric breakdown. The bipolar nature of the signal is indicative of charge creation and movement.

Figs. 2 and 3 show the von Laue plot of τ_A , which corresponds to the initial formation of the virtual anode, for 3 and 5 mm apertures at different pressures. For an exponential distribution, the slope of the data points in the von Laue plot is directly related to the inverse of the jitter and the intercept on the unit probability line is related to the characteristic time interval [8]. It can be seen in Fig. 2(a) that both the characteristic time and the jitter decrease with increasing pressure at the lower pressure range. Comparing previous results [8] in the absence of an effective hollow cathode, the data suggests that the initial ionization formation is favored by the presence of the hollow cathode. In Fig. 2(b), the same pressure dependence is no longer observed. Progressively above 200 mTorr, the initial ionization formation process appears to be increasingly random. The 5 mm aperture data in Fig. 3(a) shows the same pressure dependence as the 3 mm aperture at low pressure, but the transition to increased randomness in initial ionization formation with increasing pressure is much more prominent at the higher pressure end as shown in Fig. 3(b).

Figs. 4 and 5 show the statistics of τ_B , which corresponds to the propagation of the virtual anode from probe No. 1 to probe No. 4, for 3 and 5 mm apertures. For most of the pressure range and regardless of the cathode aperture, the time distributions follow a new trend. In general the distribution is found to fit better with a Gaussian envelope. With a Gaussian distribution, the characteristic time is given by the 50% cumulative data point on the von Laue plot, with the one σ value given by the time between the 16% and 50% cumulative data point. From the data, the characteristic time is seen to decrease with increasing pressure. The 3 mm aperture characteristic kinks are observed in the time interval distributions at low pressures, which might be attributed to a double humped distribution. A transition to increased randomness is again observed at 400 mTorr, for the 3 mm aperture. Following the trend observed for τ_A , the characteristic value of τ_B is smaller with a 3 mm diameter than a 5 mm diameter aperture.

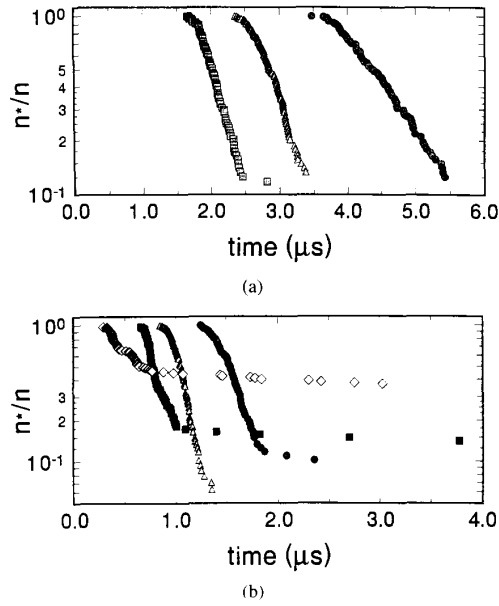


Fig. 2. von Laue plot of τ_A for a 3 mm cathode aperture at pressures of (a) \bullet 75 mTorr, \blacktriangle 100 mTorr, \blacksquare 125 mTorr and (b) \bullet 150 mTorr, \blacktriangle 200 mTorr, \blacksquare 300 mTorr, and \blacklozenge 400 mTorr. For a particular value of τ_A , n^* is the total number of discharges having a value of τ_A larger than that value. Thus n^*/n , where n is the total number of discharges, gives the cumulative probability of discharges having a certain value of τ_A .

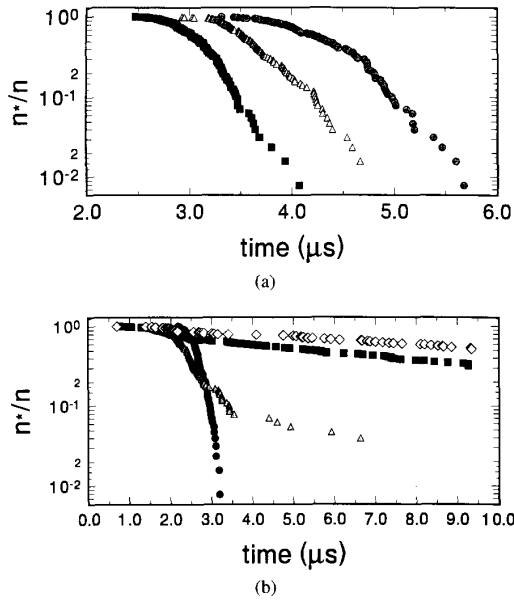


Fig. 3. von Laue plot of τ_A for a 5 mm cathode aperture at pressures of (a) \bullet 75 mTorr, \blacktriangle 100 mTorr, \blacksquare 125 mTorr and (b) \bullet 150 mTorr, \blacktriangle 200 mTorr, \blacksquare 300 mTorr, and \blacklozenge 400 mTorr.

Figs. 6 and 7 show the statistics of τ_C , which corresponds to the propagation of the virtual anode from probe No. 4 to probe No. 6. The main features of the time interval distribution follow the same trends as in Figs. 4 and 5. For both apertures, the time interval distribution curve at the lowest pressure is

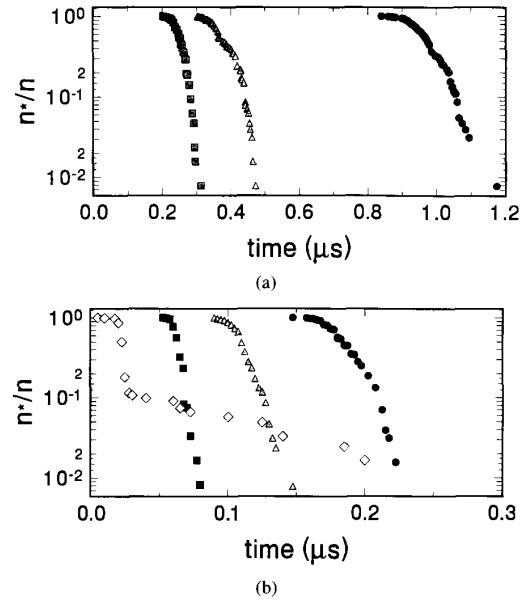


Fig. 4. von Laue plot of τ_B for a 3 mm cathode aperture at pressures of (a) \bullet 75 mTorr, \blacktriangle 100 mTorr, \blacksquare 125 mTorr and (b) \bullet 150 mTorr, \blacktriangle 200 mTorr, \blacksquare 300 mTorr, and \blacklozenge 400 mTorr.

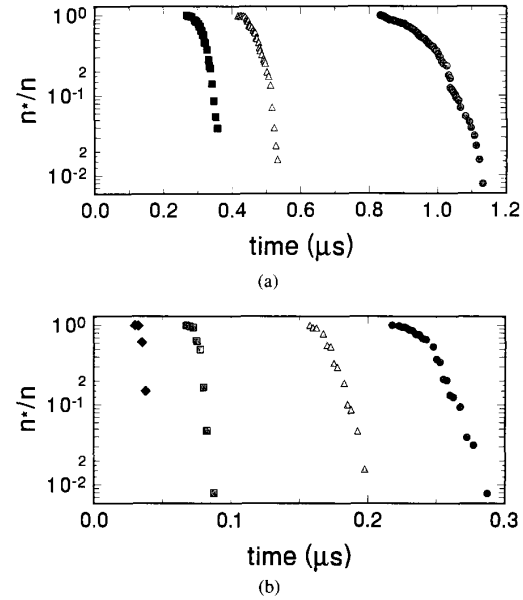


Fig. 5. von Laue plot of τ_B for a 5 mm cathode aperture at pressures of (a) \bullet 75 mTorr, \blacktriangle 100 mTorr, \blacksquare 125 mTorr and (b) \bullet 150 mTorr, \blacktriangle 200 mTorr, \blacksquare 300 mTorr, and \blacklozenge 400 mTorr.

seen to cross over another curve for a higher pressure at some point, suggesting that below certain pressure, the movement of the virtual anode is actually faster, for some of the discharges, as the pressure is reduced. This is partly the result of a change in the shape of the virtual anode signal from an exponentially rising form to a double humped form at low pressure, as shown in Fig. 8 for 5 mm aperture at 75 and 100 mTorr. There is also

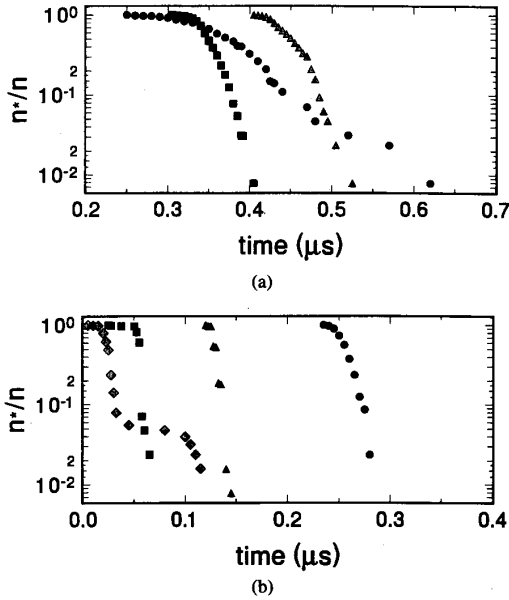


Fig. 6. von Laue plot of τ_C for a 3 mm cathode aperture at pressures of (a) 75 mTorr, 100 mTorr, 125 mTorr, 150 mTorr, 200 mTorr, 300 mTorr, and 400 mTorr.

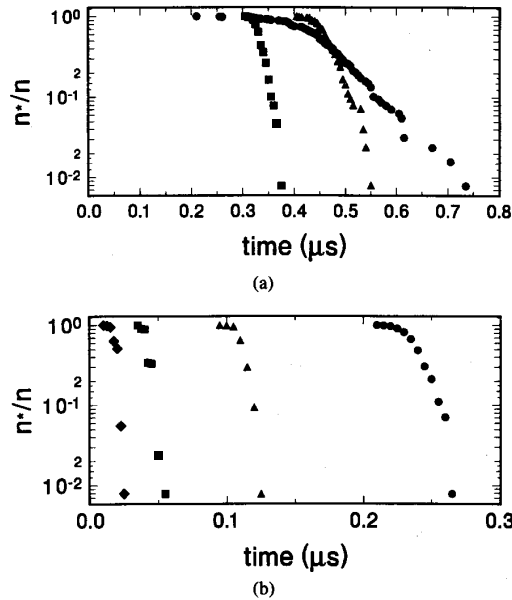


Fig. 7. von Laue plot of τ_C for a 5 mm cathode aperture at pressures of (a) 75 mTorr, 100 mTorr, 125 mTorr, 150 mTorr, 200 mTorr, 300 mTorr, and 400 mTorr.

a genuine broadening of the signal at probe 6 together with a shift of the peak to an earlier time. The definition chosen here to use the maximum of the signal as a timing point leads to an increase in τ_B with an associated decrease in τ_C , leading to the cross over observed. This variation in shape of the probe signal leads to the larger scatter of τ_C at 75 mTorr.

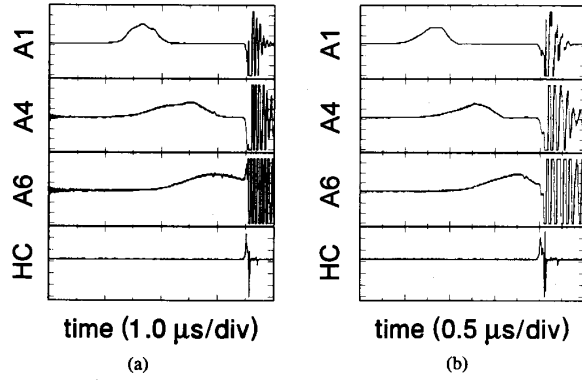


Fig. 8. Capacitive probe array signals showing the changing structure of the virtual anode formation for a 5 mm cathode aperture at 75 and 100 mTorr. The positions of the probes measured from the anode are: A1–24 mm, A4–57 mm and A6–81 mm. Probe HC is located inside the hollow cathode region close to the back of the cathode.

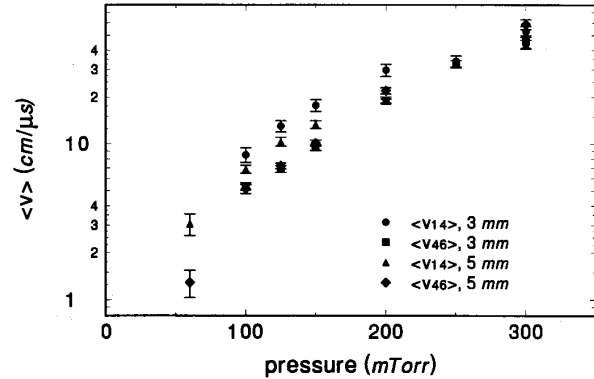


Fig. 9. Mean velocity of the virtual anode between probe 1 and probe 4, $\langle v_{14} \rangle$, and between probe 4 and probe 6, $\langle v_{46} \rangle$, as a function of pressure.

The data for τ_B and τ_C can be used to derive a mean velocity of the virtual anode between the positions of the probes. This is shown in Fig. 9 for the 3 and 5 mm diameter apertures as a function of the operating pressure. The mean virtual anode velocity increases by an order of magnitude from $50 \text{ cm} \cdot \mu\text{s}^{-1}$ at 100 mTorr to $500 \text{ cm} \cdot \mu\text{s}^{-1}$ at 300 mTorr. For a given pressure, the mean velocity of the virtual anode is not significantly different for the two aperture diameters considered. Between 100–200 mTorr, the velocity is observed to be decreasing as the virtual anode is moving closer to the cathode. At higher pressure and larger cathode aperture, there is an apparent speeding up of the virtual anode. The effect of the change in shape of the probe signal mentioned above also leads to a speeding up at low pressure.

Figs. 10 and 11 show the statistics of τ_D , which corresponds to the time delay between of the arrival of the virtual anode close to the cathode and final electric breakdown. In this case the form of the statistical distribution varies significantly over the pressure range studied. For most pressures, the distribution does not fit a simple Gaussian nor exponential function and the suggestion of a bimodal distribution for the time intervals at low pressures becomes more evident, particularly with the 3 mm aperture. The characteristic time and the slope of the time

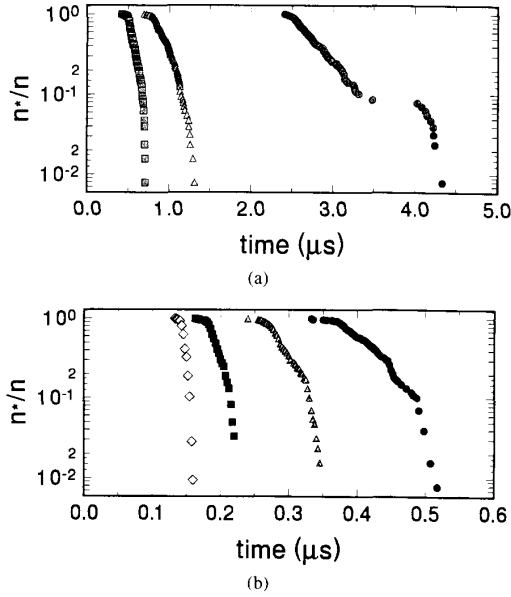


Fig. 10. von Laue plot of τ_D for a 3 mm cathode aperture at pressures of (a) \bullet 75 mTorr, \blacktriangle 100 mTorr, \blacksquare 125 mTorr and (b) \bullet 150 mTorr, \blacktriangle 200 mTorr, \blacksquare 300 mTorr, and \blacklozenge 400 mTorr.

distributions decrease monotonically with increasing pressure. In contrast to other time intervals, for the same pressure, the characteristic time obtained with the 5 mm aperture is now smaller than that with the 3 mm aperture. This difference becomes larger at lower pressure, being a factor of 2 at 125 mTorr and increasing to a factor of 3.5 at 75 mTorr.

IV. DISCUSSION

A. Statistics of Breakdown Formation

Traditionally in breakdown formation, a statistical time lag and a formative time lag can be defined to characterize the time evolution of the ionization process. The statistical time lag is defined as the time between voltage rise and the instant at which the necessary initiating electrons for ionization growth are established in the A-K gap. The formative time lag is the time interval between the appearance of the initiating electrons and full electric breakdown, as defined by the rise of the main discharge current to a specific value. The series of events responsible for establishing the condition which is sufficient for the initiation of ionization growth are essentially random, and the associated probability of an initiating event occurring in a particular time interval is described by an exponential function [13]. In general, if the mean rate of occurrence of the initiating events is ν , then the mean statistical time lag is given by $1/\nu$. On the other hand, the subsequent charge multiplication processes which lead to full ionization are probabilistic and their characteristic time, the formative time, is better described by a normal distribution.

At high pressure, collisional ionization is effective and the appearance of a seed electron would lead to breakdown through electron avalanche. In general, the formative time

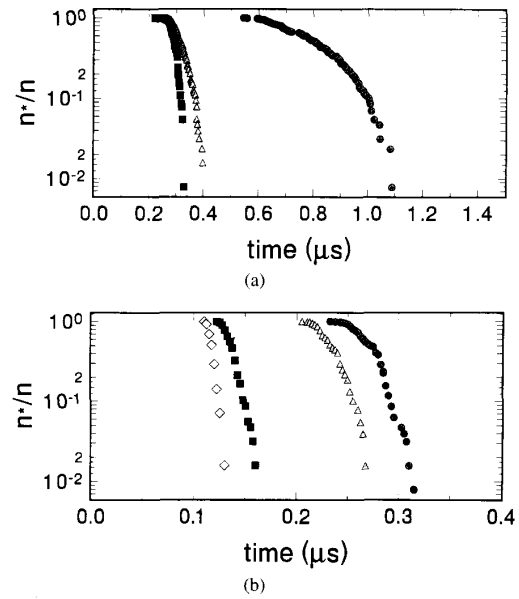


Fig. 11. von Laue plot of τ_D for a 5 mm cathode aperture at pressures of (a) \bullet 75 mTorr, \blacktriangle 100 mTorr, \blacksquare 125 mTorr and (b) \bullet 150 mTorr, \blacktriangle 200 mTorr, \blacksquare 300 mTorr, and \blacklozenge 400 mTorr.

lag is much smaller than the statistical time lag and the total time delay between the application of the voltage and breakdown is dominated by the statistical time lag. At low pressure, the ionization mean free path of electrons can be much greater than the electrode separation and the probability of an ionizing collision for an electron undergoing acceleration in the A-K gap becomes less than unity. Under this situation, the appearance of the initiating electrons no longer satisfy the condition which leads directly to sustained ionization growth and breakdown. Instead the breakdown formation would be the result of a collection of a series of different ionization growth phenomena and, as such, there may not be a simple and clear distinction between the statistical and formative times as defined traditionally.

In high over-voltage breakdown at low pressure, the breakdown often occurs on time scales not exceeding one or two electron transit time across the electrode gap. Streamer breakdown mechanism is clearly inappropriate to describe the discharge formation under such conditions. The model of virtual anode formation and movement by Lucas provides the possible solution [14]. Rather than a single avalanche as in higher pressure where space charge formation at midgap would lead to anode directed and cathode directed streamers [15], in Lucas' description, avalanche multiplication continues until the local field at the head of the avalanche reaches zero, with the subsequent formation of a neutral field free plasma between this zero field point and the anode. Further repetition of the avalanche process in the modified field between the cathode and the newly created virtual anode thus causes the position of the virtual anode, which Lucas referred to also as the tip of the streamer, to propagate towards the cathode. Only a few waves of such avalanches are required to carry the

virtual anode across the whole anode cathode gap. Breakdown is assumed to occur once the virtual anode reaches the cathode. The model was successful in predicting the rapid breakdown time at moderately low pressure though it requires a finite number of electrons being released from the cathode in a pre-defined manner to initiate the whole breakdown process. As the formation of the virtual anode is a deterministic process, it would suggest that the statistical time is associated with the creation of the necessary condition for a given number of initiating electrons to be present simultaneously.

The presence of the hollow cathode region clearly modifies the whole discharge process. On the most basic level, it could be considered as a source for the creation and supply of electrons for the main discharge region. The effect of the ions would normally be in the production of secondary electrons from the cathode surface to sustain the ionization growth process. With an effective coupling between the main A-K gap and the HCR, the ions can contribute directly and indirectly to the growth of ionization inside the HCR, through secondary electron production and space charge effect, and thus influence the rate of injection of electrons into the main gap. The role of an effective hollow cathode in the THCD could therefore be considered as one which effectively minimizes the initial statistical time in breakdown formation through enhanced production and injection of electron into the A-K gap.

B. Formation of Virtual Anode

From the data obtained, it would appear that the processes which lead to the creation of the virtual anode are more favorable with the 3 mm aperture than with the 5 mm aperture. This would suggest that despite the higher leakage field inside the HCR created by the 5 mm aperture, the overall condition is actually less efficient to create initially the condition necessary for the growth of the space charge region in the A-K gap which leads to the formation of the virtual anode.

One possible explanation for this observation lies in the concentration of electrons. For the given geometry of the hollow cathode, practically all electrons created initially inside the HCR would be expected to drift along the field lines originating from the A-K gap and be extracted into the A-K gap region. As long as the differences in the aperture diameter is such that sufficient ionization condition is still created inside the HCR as a result of the leakage field for the smaller aperture diameter cathode, the smaller aperture may in fact lead to a high electron current density in the A-K gap for the same number of extracted electrons from the HCR. Assuming that the ionization rate in the A-K gap remains the same, this would lead to a higher concentration of positive ions being produced in the main gap. These ions gain energy in the A-K gap and would return into the HCR as fast ions, thereby enhancing the ionization rate inside the HCR. Given a higher electron and ion flux, it is therefore not unreasonable to expect a more efficient overall ionization growth leading to the creation of the virtual anode, provided that the smaller aperture does not limit the field penetration inside the HCR significantly.

The increase in randomness associated with the increase in operating pressure can also be explained from the ionization

processes within the HCR. At the much lower E/N value created inside the HCR, the ionization coefficient, α , decreases almost linearly with decreasing E/N . For a given electric field penetration, it is therefore to be expected for α to fall with increasing pressure.

This argument ignores the contribution of further ionization growth in the A-K gap. When the pressure is increased beyond the point when the ionization mean free path of an electron extracted from the cathode becomes comparable to the dimension of the A-K gap, the increased efficiency in ionization from the injection of a single electron would then lead to the condition of increasing number of fast ions returning into the HCR and hence enhanced ionization growth in the HCR. In simulation on the ionization growth within the HCR, it is the additional contribution from fast ions, created through more effective ionization in the A-K gap, which leads to the reduction in overall delay to breakdown with increasing pressure. The observation here at pressures below 150 mTorr agrees with this description. At higher pressure, it would appear that the enhancement due to more effective collisional ionization in the main gap is now counteracted by the reduced ionization growth factor within the HCR.

The rapid change to a condition of large randomness with increasing pressure, where the role of the HCR is clearly no longer effective, perhaps best illustrates the delicate role of the cathode aperture and the intimate coupling between the ionization growth inside the HCR and that in the A-K gap. Between 150 and 300 mTorr, the jitter increases by more than an order of magnitude with the 5 mm aperture while that for the 3 mm aperture remains unchanged. The higher E/N introduced by the 5 mm aperture over that of the 3 mm aperture is clearly not a sufficient condition for effective control of the first step in the initiation of ionization growth in THCD.

C. Movement of the Virtual Anode

The statistics of the movement of the virtual anode show a very different picture compared with their formation. The small differences in the velocity measured with the two different aperture diameters would suggest that the HCR plays a lesser role. The initial velocity of the virtual anode is slightly faster with a 3 mm cathode aperture. The shape of the signal detected indicates that the virtual anode potential is established more readily with the smaller aperture. However, this effect is completely over-shadowed by the dependence with pressure.

In Lucas model, the velocity of the virtual anode, is directly related to the rate of electron emission from the cathode, as well as the nature of the $\alpha(E/N)$ curve. The statistics for the formation of the virtual anode established that the HCR process is more efficient with the smaller cathode aperture. The statistics of τ_B and τ_C suggest that, while this is still present in the processes which lead to the movement of the virtual anode, the effect is relatively small despite the strong dependence of the virtual anode velocity on the electron emission rate from the cathode as predicted by Lucas. On the other hand, the strong dependence on pressure for the virtual anode velocity is quite the opposite to that observed in the initial formation, particularly at the high pressure end. This suggests that the

movement is dominated by the ionization events in the main gap region, controlled by the local value of α in the space charge field, and is less dependent on the coupling to the HCR.

The statistical distribution of the time for the propagation of the virtual anode exhibits a much more deterministic nature compared with that associated with the initial formation. This leads to the near Gaussian distribution observed under some of the operating pressures. While there are only small differences in the characteristic value and the standard deviation recorded for the two aperture diameters, the actual speed with which the virtual anode is established at a given position is vastly different, being faster with the smaller aperture. With the higher and lower end of the pressures investigated, the shape of the probe signals recorded indicate that the processes responsible for the propagation of the virtual anode becomes more complex. This is also reflected in the statistics and illustrates that effects other than those occurring in the main gap might once again be important.

D. Final Breakdown

The final period of ionization growth, between the arrival of the virtual anode at the cathode and the establishment of a fully conducting channel, presents a totally different picture from that of the earlier period. The dependence on the diameter of the cathode aperture reverses, with much shorter time to breakdown recorded for the 5 mm diameter case, particularly as the operating pressure is lowered.

The shape of the probe signal is also very different for the two apertures. At 3 mm diameter, the virtual anode is fully established at probe 6 while the processes leading to the final breakdown is gradually being established. However, with the 5 mm diameter aperture, the signal indicates that though it takes longer to build up the virtual anode, the establishment of a sufficiently conducting channel across the A-K gap is happening at the same time and breakdown occurs before the signal on probe No. 6 returns to the zero point. It would appear that while an enhanced electric field is established inside the HCR with the 3 mm aperture, the enhancement is not sufficient to lead to an accelerated growth when compared with 5 mm.

The value of τ_D in fact includes two events; the propagation of the virtual anode from the position of probe 6 to the cathode, and the establishment of the necessary conditions for self-sustained current flow. If one were to subtract the propagation time from τ_D , using the projected value from τ_C , one would see an even stronger contrast between the data for the 3 and 5 mm aperture. There is a clear waiting period between the projected arrival of the virtual anode at the cathode and the final breakdown for the 3 mm aperture, increasing rapidly with decreasing pressure. While for the 5 mm aperture, for most of the pressures investigated, the value of τ_D is actually smaller than that of τ_C , indicating that the final breakdown formation processes must take place while the virtual anode is still being established some distance away from the cathode.

On a simplistic level, this difference could be explained by the much more effective field penetration with a larger diameter aperture when the anode potential is brought very close to the aperture itself. Simulation suggests that with a

suitably large aperture the whole of the anode potential could be brought inside the HCR, creating a thin sheath over the whole surface inside the HCR. The possible effect of this sheath is not investigated in this work. The studies of the electron beam evolution during this period indicate that the final breakdown is associated with the creation and injection into the A-K region of a high intensity beam [16].

The complex structure of the statistical distribution, however, indicates that there are more than one competing processes taking place in the final stage of discharge formation. Two distinct slopes can be identified in many of the distribution curves; one associated with a small jitter but large value of the characteristic time, and the other with a larger jitter but a smaller characteristic time. There is no increase in randomness at the higher pressure end in the statistics, suggesting that the ionization phenomena is primarily dominated by growth at high E/N .

V. SUMMARY AND CONCLUSION

From the statistical distribution of the virtual anode signals, breakdown formation at low pressure in a transient hollow cathode discharge can clearly be separated into three distinct regimes of ionization growth; 1) the initiation of ionization growth leading to the formation of a plasma region close to the anode, 2) the extension of this plasma region towards the cathode and 3) the ionization growth within the hollow cathode region under the much enhanced field as the anode potential is brought close to the cathode. The regime 1) is essentially random in nature, and the time delay between the application of an over-voltage and the onset of this condition is strongly influenced by primary and secondary events taking place within the HCR. The size of the cathode aperture, which determines both the E/N condition inside the HCR and the degree of coupling with the A-K gap, has strong influence in shaping the statistics of the delay in this regime. As the data for the 5 mm diameter aperture has shown, simply increasing the local value of E/N in the HCR would not lead to a higher probability of initiation at this stage and the smaller 3 mm aperture in fact leads to a more optimum condition and thus shorter time delay. The regime 2) is highly deterministic and is associated uniquely with ionization growth within the A-K gap region. During this period a plasma region is formed between the anode and cathode region but the overall conductivity of this channel is such that it does not necessarily lead to the condition required for the collapse of plasma resistance and high current growth. The formation and movement of the virtual anode is assisted by the continuous injection of electrons from the HCR. The dimension of the cathode aperture has much less influence in this regime except towards the end, when the anode potential is brought near to the cathode, and thus modifying greatly the electric field strength inside the HCR. Regime 3) represents ionization events which take place primarily within the HCR under strongly modified field conditions. Events which are necessary to increase the electron density in the conducting channel to a value which would sustain a high current growth. Within the HCR, the size of the cathode aperture determines how quickly

the local E/N will grow. The larger 5 mm aperture data shows that the final breakdown processes are taking place while the virtual anode is still being set up some distance away from the cathode surface in the main gap. Unlike previous regimes, the smaller 3 mm aperture leads to slower breakdown formation, particularly at low operating pressures. The statistics indicate that there are more than one competing ionization processes taking place though the origin of these processes could not be inferred from the data. The growth of a localized space charge within the HCR in the final part of this regime is measured but there are insufficient details to treat the data using the current method. The presence of such space charge would lead to enhanced localized ionization growth and the correlation of this feature with the formation of an enhanced electron beam is discussed elsewhere [16]. Further studies are underway to extend the statistical analyses to include both the space charge signal within the HCR and the electron beams.

ACKNOWLEDGMENT

M. Favre acknowledges the support of a Marie Curie Fellowship awarded by the Commission of the European Communities (CEC) for the visit to Imperial College.

REFERENCES

- [1] J. P. Boeuf and L. Pitchford, "Pseudospark discharges via computer simulation," *IEEE Trans. Plasma Sci.*, vol. 19, p. 286, 1991.
- [2] P. Choi, R. Aliaga, B. Blottiere, M. Favre, J. Moreno *et al.*, "Experimental studies of ionization processes in the breakdown phase of a transient hollow cathode discharge," *Appl. Phys. Lett.*, vol. 63, p. 2750, 1993.
- [3] K. Mittag, P. Choi, and Y. Kaufman, "Modelling of the hollow cathode plasma for the pre-breakdown phase of a pseudospark discharge," *Nucl. Instrum. Method A*, vol. 292, p. 465, 1990.
- [4] P. Choi, H. Chauqui, J. Lunney, R. Reichle, A. J. Davies, and K. Mittag, "Plasma formation in a pseudospark discharge," *IEEE Trans. Plasma Sci.*, vol. 17, p. 770, 1989.
- [5] M. Favre, H. Chauqui, E. Wyndham, and P. Choi, "Measurements on electron beams in a pulsed hollow cathode discharge," *IEEE Trans. Plasma Sci.*, vol. 20, p. 53, 1992.
- [6] K. Frank and J. Christiansen, "The fundamentals of the pseudospark and its applications," in *Proc. XIII Int. Symp. Discharges Elec. Insulation in Vacuum*, Paris, France, 1988, p. 367.
- [7] K. K. Jain, E. Boggasch, M. Reiser, and M. J. Rhee, "Experimental investigation of the pseudospark-produced high-brightness electron beam," *Phys. Fluids B*, vol. 2, p. 2487, 1990.
- [8] P. Choi and R. Aliaga, "A statistical study of the transient hollow cathode discharge," in *Proc. Int. Conf. Gas Discharges*, Swansea, U.K., 1992, p. 792.
- [9] P. Choi, Y. Kaufman, and R. Aliaga, "Role of long-lived species in pulsed hollow cathode discharges in N_2 ," *Appl. Phys. Lett.*, vol. 57, p. 440, 1990.
- [10] M. Favre, A. M. Lefiero, P. Choi, H. Chauqui, and E. Wyndham, "Dependence of cathode aperture in pulsed hollow cathode discharges," *Appl. Phys. Lett.*, vol. 60, p. 32, 1992.
- [11] P. Choi and M. Favre, "A capacitive probe array for measurements of ionization growth," *Rev. Sci. Instrum.*, vol. 65, p. 2281, 1994.
- [12] M. von Laue, "Bemerkung zu K. Zubers Messung der Verzögerungszeiten bei Funkenentladung," *Ann. Phys.*, vol. 76, p. 721, 1925.
- [13] F. Lewellyn Jones and E. T. de la Perrelle, "Field emission of electrons in discharges," *Proc. R. Soc. A*, vol. 216, p. 267, 1953.
- [14] J. Lucas, "A theoretical and experimental study of short duration breakdown times in low pressure gases," in *Proc. 5th Int. Conf. on Phenomena in Ionized Gases*, Munchen, Germany, 1961, p. 693.
- [15] S. J. Levinson and E. E. Kundhart, "Investigation of the statistical and formative time lags associated with the breakdown of a gas in a gap at high voltage," *IEEE Trans. Plasma Sci.*, vol. PS-10, p. 266, 1982.
- [16] M. Favre, P. Choi, H. Chauqui, J. Moreno, E. Wyndham, and M. Zambra, "Hollow cathode effects in charge development processes in the transient hollow cathode discharge," *IEEE Trans. Plasma Sci.*, pp. 212-220, this issue.

P. Choi, photograph and biography not available at the time of publication.

H. Chauqui, photograph and biography not available at the time of publication.

M. Favre, photograph and biography not available at the time of publication.

V. Colas, photograph and biography not available at the time of publication.